

Finite element simulation of viscoelastic flow through a converging channel

G. Rekers, R. Akkerman & J. Huétink

University of Twente, Department of Mechanical Engineering

P.O. Box 217, 7500AE Enschede, The Netherlands

ABSTRACT: A number of well-known nonlinear viscoelastic constitutive models of the differential type are fitted within the theory of irreversible thermodynamics. Two of these models, the Leonov model and the Giesekus model, are used to describe the flow behaviour of an LDPE and an HDPE in a converging slit channel. These constitutive models have been implemented in a transient finite element code using an Arbitrary Lagrange-Euler method, being particularly suitable for the description of history dependent processes involving free surface movements. Some occurring numerical problems are shortly discussed, such as an objectivity preserving numerical integration scheme. Finally, the calculated flow induced stresses are compared to the stress fields measured using flow induced birefringence.

1 INTRODUCTION

Various differential constitutive equations are formulated to describe the nonlinear viscoelastic behaviour of an initially isotropic polymer melt. All models have the same linear visco-elastic limit, but exhibit differences in the nonlinear viscoelastic region. This nonlinear behaviour plays an important role in polymer processing. For instance, the flow induced residual stresses in injection moulded products, caused by nonlinear viscoelastic flow during the injection, have a large influence on for example the mechanical, thermal and optical properties of the finished product (Baaijens et al. 1991). The nonlinear behaviour is also important in many other processes, as e.g. film blowing (Tas 1994) and extrusion (Goublomme et al. 1992).

2 CONSTITUTIVE EQUATIONS

To describe the instationary behaviour of a highly viscous fluid (low Reynolds numbers) use is made of the mechanical equilibrium, in absence of body forces stating

$$\sigma \cdot \nabla = \mathbf{0}. \quad (1)$$

For the description of polymer melts and solutions often the generalized Jeffreys model is used, in

which a number of Maxwell modes is connected in parallel with a Newtonian viscosity. By using a set of Maxwell elements a set of relaxation times can be described. Usually, the viscous damper is only temperature dependent and does not depend on the deformation. In the remaining part of this section firstly the kinematics and the basic model assumptions of a single Maxwell mode are discussed. Secondly, a number of well-known constitutive models describing incompressible nonlinear viscoelastic behaviour is fitted into this formulation.

To incorporate the nonlinear viscoelastic behaviour in the continuum mechanics approach, for each Maxwell mode, besides the reference and current configuration, the relaxed configuration (Leonov 1976) or natural reference state (Besseling 1968) is introduced to make it possible to determine the reversible part of the deformation of each Maxwell mode. Using this assumption the deformation gradient \mathbf{F} can multiplicatively be decomposed into a reversible (elastic) part \mathbf{F}_e and an irreversible (plastic) part \mathbf{F}_p : $\mathbf{F} = \mathbf{F}_e \cdot \mathbf{F}_p$. Thereupon an objective elastic strain measure can be defined in the shape of the elastic Finger tensor $\mathbf{B}_e = \mathbf{F}_e \cdot \mathbf{F}_e^T$. The evolution of the elastic Finger strain is found to be

$$\begin{aligned}\dot{\mathbf{B}}_e &= \mathbf{L}_e \cdot \mathbf{B}_e + \mathbf{B}_e \cdot \mathbf{L}_e^T \\ &= (\mathbf{L} - \mathbf{D}_p) \cdot \mathbf{B}_e + \mathbf{B}_e \cdot (\mathbf{L}^T - \mathbf{D}_p^T),\end{aligned}\quad (2)$$

in which \mathbf{L} is the gradient of velocity tensor, \mathbf{L}_e is the elastic part of the gradient of velocity tensor and \mathbf{D}_p is the plastic part of the rate of deformation tensor.

In order to model compressible nonlinear viscoelastic material behaviour we want the isotropic deformations to be elastic and only the deviatoric deformations to be viscoelastic. When $tr\mathbf{D}_p=0$ the evolution equation for \mathbf{B}_e also describes the law of mass conservation, but when $tr\mathbf{D}_p \neq 0$ the density variations are not described by the elastic Finger strain \mathbf{B}_e anymore. Therefore, the strain split of the elastic Finger strain proposed by Huétink (1986) is introduced

$$\mathbf{B}_e^r = \mathbf{B}_e - J_e^{2/3} \mathbf{1}, \quad (3)$$

in which $J_e = \det(\mathbf{F}_e)$. In case of purely isotropic deformations $\mathbf{B}_e^r = \mathbf{0}$. At this point the basic assumption of the theory of Leonov (1976) is introduced, which states that in polymeric liquids there always exists an 'elastic limit', a quasi-equilibrium situation is achieved on very rapid (instantaneous) deformations. Therefore, we suppose the thermodynamic state variables to be \mathbf{B}_e^r , $J = \det(\mathbf{F})$ and T . Furthermore, a purely isotropic part is splitted from the free energy:

$$\Psi(\mathbf{B}_e, J, T) \equiv \Psi_d(\mathbf{B}_e^r, T) + \Psi_v(J, T). \quad (4)$$

In case of rubber elasticity, the free energy function describing non-isotropic deformations is

$$\begin{aligned}\Psi_d(\mathbf{B}_e^r, T) &= \frac{RT}{M_e} I_{\mathbf{B}_e^r} \\ &= \frac{\mu(\rho, T)}{2\rho} (I_{\mathbf{B}_e} - 3J_e^{2/3}),\end{aligned}\quad (5)$$

in which

$$I_{\mathbf{B}_e} = tr(\mathbf{B}_e)$$

The shear modulus μ is a function of the temperature T and the density ρ :

$$\mu(\rho, T) = \frac{\rho T}{\rho(T_{ref})T_{ref}} \mu_{ref} = c_T \mu_{ref}. \quad (6)$$

Using the quasi-equilibrium approach the constitutive equation can be worked out to

$$\boldsymbol{\sigma}(\mathbf{B}_e^r, J, T) = c_T \mu_{ref} \mathbf{B}_e^r - p(J, T) \mathbf{1}, \quad (7)$$

in which $p(J, T)$ can be specified without knowing the free energy function

$$\dot{p} = -C_b tr(\mathbf{D}) + \alpha C_b \dot{T}, \quad (8)$$

in which α is the coefficient of thermal expansion and C_b is the bulk modulus. These parameters can be taken constant, but they can also be assumed to be a function of the temperature and the determinant of the deformation tensor J . The isotropic deformation is thus modelled as being time independent.

To complete the description the plastic rate of deformation has to be specified. By using different definitions for the plastic deformation rate a number of well-known constitutive equations can be found (Leonov 1992):

Upper Convected Maxwell (UCM) model

$$\mathbf{D}_p = -\frac{1}{2\theta} (\mathbf{B}_e^{-1} - \mathbf{1}). \quad (9)$$

Leonov model

$$\mathbf{D}_p = \frac{1}{4\theta} (\mathbf{B}_e - \mathbf{B}_e^{-1})^d. \quad (10)$$

Giesekus model

$$\mathbf{D}_p = \frac{1}{2\theta} \left(\alpha (\mathbf{B}_e - \mathbf{1}) - (1-\alpha) (\mathbf{B}_e^{-1} - \mathbf{1}) \right). \quad (11)$$

In this equation is θ the relaxation time and the parameter α in the Giesekus model is a numerical fitting parameter introduced to get a better description of the nonlinear material behaviour. Note that it is also possible to incorporate the upper convected version of the Phan-Thien Tanner (PTT) model in our formulation. The PTT model including the Gordon-Showalter convected time derivative cannot be included, because it is totally non-equilibrium.

In this paper only isothermal polymer flow is

considered, but non-isothermal flow can simply be incorporated in the description above, so the free energy is specified for the constitutive models used.

To obtain a good description of the rheological behaviour of the LDPE and HDPE melts, it is necessary to introduce a multi-mode approach. The nonlinear relaxation properties can be described by a set of mutually non-intersecting relaxation modes,

$$\boldsymbol{\sigma} = -p\mathbf{I} + \sum_{i=1}^n \boldsymbol{\sigma}_{M,i}, \quad (12)$$

in which $\boldsymbol{\sigma}_{M,i}$ represents the thermodynamic stress of each Maxwell mode. When also additional viscous friction is incorporated, the generalized Jeffreys model is obtained.

3 FINITE ELEMENT FORMULATION

The constitutive models described are implemented in a transient Galerkin finite element code (updated Lagrange formulation), in which the weak form of the balance of momentum, equation (1), is approximated. By extending the updated Lagrange formulation with an Euler step, the resulting Arbitrary Lagrange Euler (ALE) formulation (Huétink 1992) can be applied to fluid flow problems as well as solid mechanics. Thus, the algorithm is based on a split Lagrangian and Eulerian step.

Every time step the evolution of the elastic Finger strain (equation (2)) has to be integrated. If any integration scheme is directly applied to this equation, incremental objectivity is not necessarily preserved. To obtain incremental objectivity the recipe of Baaijens (1993) is applied. Firstly, an invariant tensor $\bar{\mathbf{B}}_e$ corresponding with the objective tensor \mathbf{B}_e is defined

$$\bar{\mathbf{B}}_e = \mathbf{F}^{-1} \cdot \mathbf{B}_e \cdot \mathbf{F}^{-T}. \quad (13)$$

Secondly, the evolution equation (2) is rewritten by using the upper convected time derivative and by recognizing that for the constitutive models used \mathbf{D}_p is a linear function of \mathbf{B}_e and \mathbf{B}_e^{-1} :

$$\bar{\nabla} \bar{\mathbf{B}}_e = -2\mathbf{D}_p \cdot \mathbf{B}_e. \quad (14)$$

Using the invariant tensor $\bar{\mathbf{B}}_e$, the evolution equation can be elaborated to

$$\dot{\bar{\mathbf{B}}}_e = \mathbf{F}^{-1} \cdot (-2\mathbf{D}_p \cdot \mathbf{B}_e) \cdot \mathbf{F}^{-T}. \quad (15)$$

Integration of this form using a generalized midpoint rule yields

$$\frac{\bar{\mathbf{B}}_{e_{n+1}} - \bar{\mathbf{B}}_{e_n}}{\Delta t} = \mathbf{F}_{n+\alpha}^{-1} \cdot (-2\mathbf{D}_p \cdot \mathbf{B}_e)_{n+\alpha} \cdot \mathbf{F}_{n+\alpha}^{-T}. \quad (16)$$

Noting that $\dot{\mathbf{F}} = \mathbf{L} \cdot \mathbf{F}$ and assuming that $\mathbf{F}_n = \mathbf{I}$ (updated Lagrange formulation), it is proposed to calculate the deformation tensor as follows, assuming that the gradient of velocity is constant during a time step:

$$\mathbf{F}_{n+\alpha} = e^{\alpha \Delta t \mathbf{L}} = \sum_{k=0}^{\infty} \frac{(\alpha \Delta t \mathbf{L})^k}{k!}. \quad (17)$$

When $\Delta t \mathbf{L}$ is small, the series is converging and the deformation gradient can be calculated up to machine accuracy. Moreover, for the choice of $\alpha=0.5$ in equation (16) the algorithm is second-order accurate, but it has to be solved iteratively. It is also possible to combine equation (16) with a fourth-order accurate Runge Kutta method.

The convection of the elastic Finger strain \mathbf{B}_e during each time step, the Eulerian part of the algorithm, is considered independent of the integration scheme. For the simulations presented in this paper an upwind scheme is used (Akkerman 1993), but it is also possible to incorporate a more accurate convection scheme, such as the Law-Wendroff scheme or a TVD scheme using flux limiters. However, this part of the algorithm is still being investigated.

At the end of each time step the mechanical equilibrium has to be obtained. Therefore, a Newton-Raphson method is applied to solve the weak form of equation (1) (Akkerman 1993). In a finite element context it can also be said that this iterative procedure must find a zero for the vector of nodal unbalance forces.

4 FLOW IN A CONVERGING SLIT CHANNEL

For all models the relaxation time spectrum is fitted on dynamical mechanical experiments (DMS) in the linear viscoelastic region. This spectrum is independent of the model used, because in this region they predict identical behaviour. For both LDPE (Tas 1994) and HDPE (DSM Research, The Netherlands) this spectrum is

given in Table 1.

HDPE		LDPE	
θ_i (s)	μ_i (Pa)	θ_i (s)	μ_i (Pa)
1.07e-3	2.18e5	7.70e-5	2.72e5
1.13e-2	1.64e4	7.05e-4	1.05e5
7.42e-2	2.59e3	5.13e-3	6.02e4
4.71e-1	2.56e2	3.59e-2	3.16e4
2.79e0	1.96e1	2.42e-1	1.37e4
9.13e0	2.87e0	1.58e0	4.52e3
		1.01e1	1.01e3
		7.20e1	1.46e2

Table 1: Discrete relaxation time spectra for HDPE at 160°C and LDPE at 190°C.

The non-linearity parameter in the Giesekus model was obtained by fitting the results of stress build-up and relaxation experiments (LDPE) and steady shear data (HDPE). For HDPE $\alpha=0.6$ and for LDPE $\alpha=0.35$.

At DSM Research birefringence measurements were used to obtain the stress fields in a converging slit channel with the dimensions as given in Figure 1 (Tas, 1994).

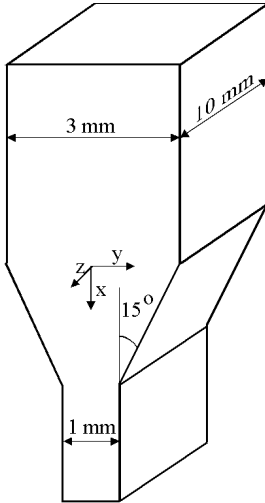


Figure 1: Geometry of the converging channel.

The experiments were carried out at 160°C for HDPE and 190°C for LDPE (De Bie et al. 1994). A more extensive description of the experimental work can be found in the graduate reports of Kikstra (1994) and De Bie (1994). In this paper the results of these measurements are used to evaluate the value of the results of the numerical simulations done with our finite element code.

In the simulations, a 2-D flow field (plane strain) is assumed with no flow in the z-direction. Because the problem is symmetric with respect to the x-axis only one half of the converging channel is modelled. The problem is meshed using bilinear interpolation 4-node isoparametric elements with

the 8 nodal displacements as degrees of freedom. To prevent volume-locking the dilatation is integrated using one integration point. The finite element mesh used is represented in Figure 2, but it is noted that the in- and outflow are only partially depicted in this figure.

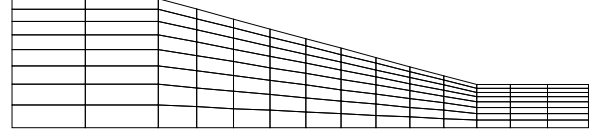


Figure 2: Part of the finite element mesh.

The boundary conditions that are used in the simulation are: stick at the wall, a prescribed velocity profile at the inflow. The inflow velocity profile has to change during the transient calculations: starting from an elasticity-free state the velocity profile develops from a parabolic profile to a flatter profile depending on the material properties and the flow rate (Rekers et al. 1993). Furthermore, incompressibility is assumed by taking a high value for the bulk modulus, i.e. $C_b=1.e10$ Pa (penalty formulation). Also, the flow is assumed to be isothermal.

The experiments for HDPE were carried out at a flow rate of 21.4mm³/s. The calculated shear stresses σ_{xy} and first normal stress differences N_1 are compared to the measurements at a cross section in the contraction, $x=2.20$ mm (Figure 3), and at a cross section in the outflow, $x=7.70$ mm (Figure 4).

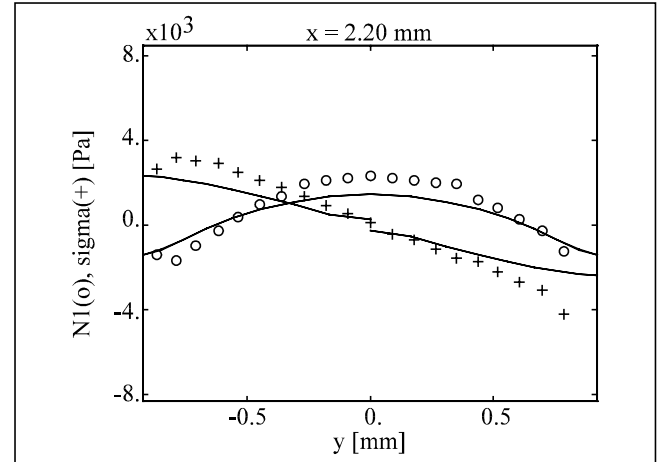


Figure 3: Measured $N_1(o)$ and $\sigma_{xy}(+)$ and calculations with Leonov(-) and Giesekus(--). for HDPE.

At the centre line, $y=0$ mm, of the converging slit the flow type is pure planar elongation. Hence, the first normal stress difference at the centre line is due to planar elongation only. Both measured and calculated N_1 are represented in Figure 5.

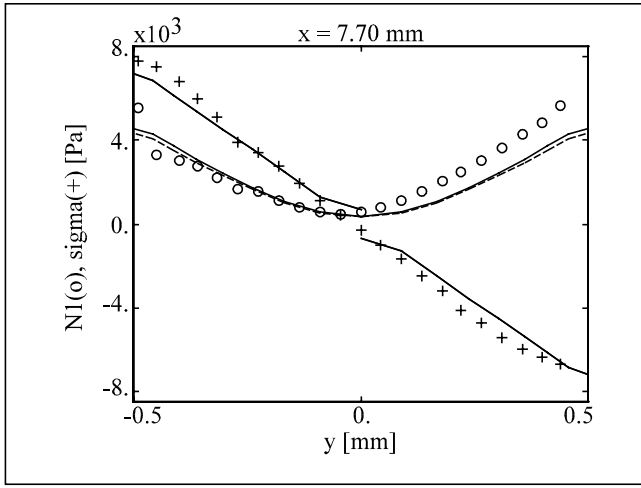


Figure 4: Measured $N_1(o)$ and $\sigma_{xy}(+)$ and calculations with Leonov(-) and Giesekus(--). for HDPE.

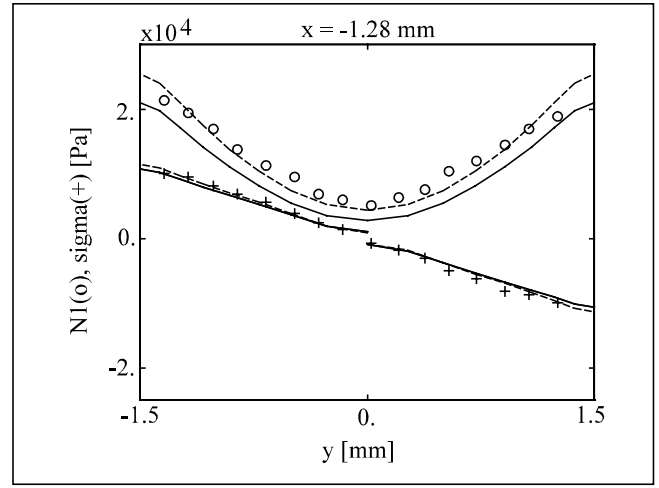


Figure 6: Measured $N_1(o)$ and $\sigma_{xy}(+)$ and calculations with Leonov(-) and Giesekus(--). for LDPE.

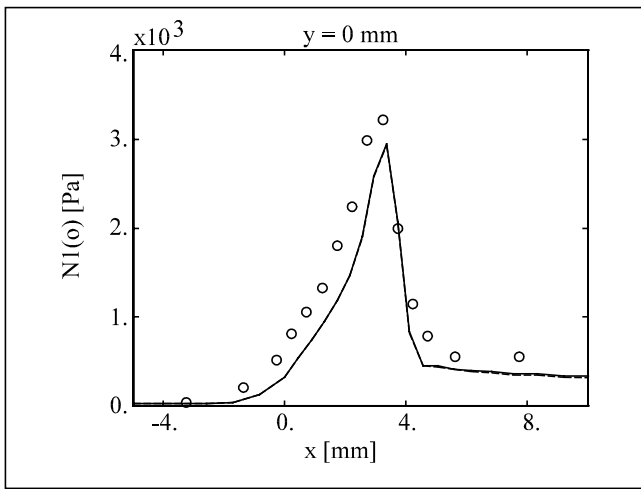


Figure 5: Measured $N_1(o)$ and calculations with Leonov(-) and Giesekus(--). for HDPE.

The experiments for LDPE were carried out at a flow rate of $17.2 \text{ mm}^3/\text{s}$. The calculated shear stresses σ_{xy} and first normal stress differences N_1 are compared to the measurements at a cross section in the inflow, $x = -1.28 \text{ mm}$ (Figure 6), at a cross section in the contraction, $x = 1.62 \text{ mm}$ (Figure 7), at a cross section in the outflow, $x = 7.32 \text{ mm}$ (Figure 8). The measured and calculated first normal stress differences at the centre line are depicted in Figure 9.

DISCUSSION AND CONCLUSIONS

For HDPE, it can be seen that both models predict nearly the same shear stresses and first normal stress differences on all points of the mesh. The predictions for the shape of the shear stresses and first normal stress differences is qualitatively very good. Quantitatively, the calculations give better results in the outflow region than in the contraction.

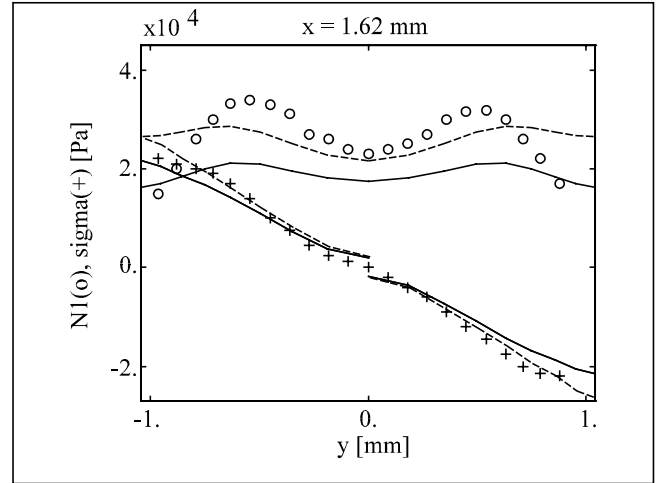


Figure 7: Measured $N_1(o)$ and $\sigma_{xy}(+)$ and calculations with Leonov(-) and Giesekus(--). for LDPE.

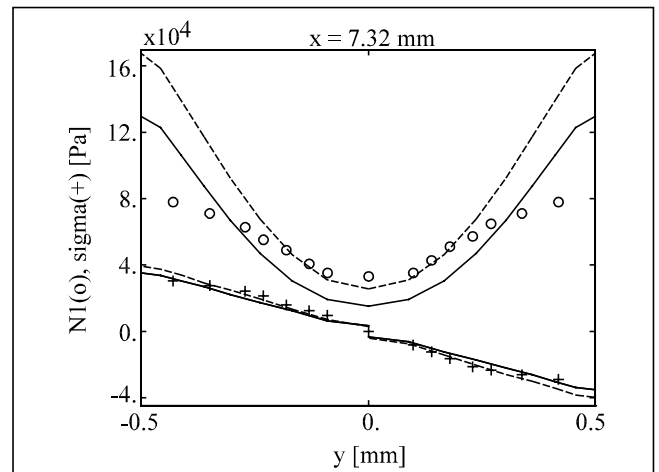


Figure 8: Measured $N_1(o)$ and $\sigma_{xy}(+)$ and calculations with Leonov(-) and Giesekus(--). for LDPE.

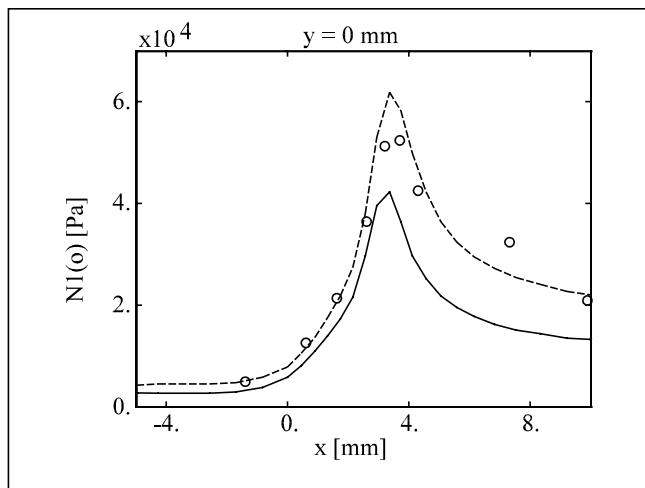


Figure 9: Measured $N1(o)$ and calculations with Leonov(-) and Giesekus(-- for LDPE.

For LDPE, it is clear that the shear stresses and the first normal stress differences are better predicted by the Giesekus model than the Leonov model. In the inflow, the predicted first normal stress differences using the Giesekus model are quantitatively in good agreement with the measurements, but in the contraction and in the outflow only qualitative agreement is obtained. A possible explanation for this difference is that in this region wall slip is present. The first normal stress differences build up along the symmetry line are quite well predicted, but at the inflow the first normal stress differences are not equal to zero, as it should be for a fully developed shear flow.

Comparing the results of HDPE and LDPE, it is observed that the LDPE exhibits a higher level of elasticity which may explain that the predictions for LDPE are less accurate than for HDPE. Comparing the shape of the predicted first normal stress difference profiles at a cross section in the contraction, for HDPE a parabolic shape is found and for LDPE a maximum is found between the wall and the centre.

Concluding this paper it can be said that the elasticity of polymeric liquids is very important for predicting its flow behaviour. For the materials and flow rates investigated the High Weissenberg Number Problem was not present, but for other materials or higher flow rates it may be present. It is observed that some of the predictions are quite good, but there is still a lot of work to be done to get quantitatively good predictions.

ACKNOWLEDGEMENTS

The support of the Dutch research programme "IOP Polymeren" and of DSM Research is gratefully acknowledged. Especially thanks to Marnix van Gulp, Arie Schepens, Han Slot and Gerard

Vlogman of DSM for our valuable discussions.

REFERENCES

- Akkerman, R. 1993. *Euler-Lagrange simulations of nonisothermal viscoelastic flows* (thesis). Enschede.
- Baaijens, F.P.T. & L.F.A. Douven 1991. Calculation of flow-induced residual stress in injection moulded products, *Applied Scientific Research* 48:141-157. Kluwer Academic Publishers.
- Baaijens, F.P.T. 1993. An U-ALE formulation of 3-D unsteady viscoelastic flow, *International Journal for Numerical Methods in Engineering* 36:1115-1143. John Wiley & Sons.
- Bie, F.O. de, P.P. Tas, W.P. Kikstra & M. van Gulp 1994. Viscoelastic flow in a converging slit channel: rheo-optical measurements and numerical simulation. *Proceedings of the Fourth European Rheology Conference* 471-473. Sevilla.
- Bie, F.O. 1994. *Visco-elastische stromingen in een convergerend kanaal: reo-optische experimenten en numerieke simulatie* (graduate report in Dutch). Eindhoven.
- Besseling, J.F. 1968. A thermodynamic approach to rheology, *IUTAM symposium of irreversible aspects of continuum mechanics 1966*:16-53. Springer Verlag.
- Goublomme, A., B. Draily & M.J. Crochet 1992. Numerical prediction of extrudate swell of a high density polyethylene, *Journal of non-Newtonian fluid mechanics* 44:171-195. Amsterdam: Elsevier Science Publishers.
- Huétink, J. 1986. *On the simulation of thermomechanical forming processes* (thesis). Enschede.
- Huétink, J. & P.N. van der Helm 1992. On Euler-Lagrange finite element formulation in forming and fluid problems, *Numerical Methods in Industrial Forming Processes* 4:45-54. Rotterdam: Balkema.
- Kikstra, W.P. 1994. *Rheo-optical measurements and numerical simulations of a HDPE flow through a converging slit channel* (graduate report). Enschede.
- Leonov, A.I. 1976. Nonequilibrium thermodynamics and rheology of viscoelastic polymer media, *Rheologica Acta* 15:85-98. Steinkopff Verlag.
- Leonov, A.I. 1992. Analysis of simple constitutive equations for viscoelastic liquids, *Journal of non-Newtonian fluid mechanics* 42:323-350. Amsterdam: Elsevier Science Publishers.
- Rekers G., R. Akkerman, J. Huétink 1993. Finite element simulations of local effects in nonisothermal viscoelastic and viscous flows. *Finite Elements in Fluids* 8: 1093-1102.
- Tas, P.P. 1994. *Film blowing: from polymer to product* (thesis). Eindhoven.